EUROPEAN FUSION DEVELOPMENT AGREEMENT

EFDA–JET–CP(04)02/08

A. Huber, J. Rapp, P. Andrew, P. Coad, G. Corrigan, K. Erents,
W. Fundamenski, L.C. Ingesson, K. Itami, S. Jachmich, A. Korotkov,
G.F. Matthews, Ph. Mertens, V. Philipps, R. Pitts, B. Schweer, G. Sergienko,
M. Stamp and JET EFDA Contributors

The Effect of Field Reversal on the JET MkIIGB-SRP Divertor Performance in L-mode Density Limit Discharges

The Effect of Field Reversal on the JET MkIIGB-SRP Divertor Performance in L-mode Density Limit Discharges

A. Huber[1], J. Rapp[1], P. Andrew[2], P. Coad[2], G. Corrigan[2], K. Erents[2], W. Fundamenski[2], L.C. Ingesson[3], K. Itami[4], S. Jachmich[1], A. Korotkov[2], G.F. Matthews[2], Ph. Mertens[1], V. Philipps[1], R. Pitts[5], B. Schweer[1], G. Sergienko[1], M. Stamp[2] and JET EFDA Contributors*

[1]*Institut für Plasmaphysik, Forschungszentrum Jülich GmbH, EURATOM Association, Trilateral Euregio Cluster,52425 Jülich, Germany*
[2]*EURATOM/UKAEA Fusion Association, Culham Science Centre, Abingdon Oxon OX14 3DB, UK*
[3]*FOM-Instituut voor Plasmafysica, Nieuwegein, The Netherlands*
[4]*Japan Atomic Energy Research Institute, Naka-machi, Ibaraki-ken, Japan 311-0193*
[5]CRPP, Association EURATOM-Confederation Suisse, EPFL, Lausanne, Switzerland
** See annex of J. Pamela et al, "Overview of Recent JET Results and Future Perspectives", Fusion Energy 2002 (Proc. 19th IAEAFusion Energy Conference, Lyon (2002).*

Preprint of Paper to be submitted for publication in Proceedings of the
16th PSI Conference,
(Portland Maine, USA 24-28 May 2004)

***A*BSTRACT**

The effect of field reversal on the JET MkIIGB-SRP divertor performance has been investigated in L-mode density limit discharges. These experiments show that the direction of the magnetic field has a substantial effect on divertor physics, modifying the character of detachment and density limits. Reversal of the ion ∇B drift direction away from the X-point results in a reduction of the density limit of about 15%. In contrast to forward field direction, the divertor parameters such as density and temperature as well as divertor radiation distribution and power at the divertor target become more symmetrical in the discharges with reversed field operation. The influence of the different field configurations on the divertor performance has been analysed with respect to the dependence on density and heating power. The experimental observations of out-in asymmetry in target power as well as in the CIII-emission distribution is consistent with EDGE2D simulations, which include the effect of drifts.

1.INTRODUCTION

Most of single-null divertor tokamak experiments show strong in-out asymmetries in particle and heat fluxes connected to asymmetries in divertor density, temperature and radiation. The analysis of these asymmetries is essential for the general understanding of divertor properties such as detachment, power exhaust, recombination, recycling and erosion/redeposition. The imbalances depend on the direction of the toroidal magnetic field and are thus most probably a result of particle cross-field drifts.

In the past, experiments have been performed in many divertor tokamaks [1-5], including JET [6,7] which show substantial effects of the field reversal on asymmetries of power to the divertor plates, plasma density and temperature as well as of radiation in the divertor. Despite numerous experiments with reversed toroidal field direction, the observations are often incomplete or must be repeated with improved diagnostics. In this paper, we describe the effect of the toroidal field reversal on divertor plasma in L-mode density limit discharges with different heating power input.

2. EXPERIMENTAL SET-UP

At JET, the spatial distribution of impurity radiation in the divertor has been analysed using three CCD cameras coupled to selectable interference filters (D_α-, CII-, CIII- emission lines. For this analysis, a 3D-tomographic reconstruction [8], reduced to a 2D-problem by the assumption of toroidal symmetry, has been performed. A survey spectrometer in the visible (KS3) provides integrated D_α-, CII- and CIII-signals over both divertor legs and is used for cross-calibration and for comparison with the reconstructed 2D distributions of the line radiation.

In addition to the spectroscopic diagnostics, there is a poloidal array of fixed Langmuir probes (KY4D) in the inner and outer divertor targets that are used to measure local saturation current, electron density and temperature.

Power leaving the plasma is measured with a bolometer system (KB1, KB3 and KB4) for the

radiated power and with an infra-red camera for the power flux to plasma-facing surfaces. The bolometer system provides complete plasma coverage and was used for tomographical reconstruction of the distribution of total radiation.

3. RESULTS AND DISCUSSION

The effect of the field direction on the divertor (Mk IIGB-SRP) performance has been investigated on JET by reversing the toroidal field and plasma current direction simultaneously, so that the magnetic helicity remained constant. For this study, L-mode density limit experiments have been performed with B_T=2.4°T, I_p=1.7°MA and with an additional NBI power of 1.0-4.5°MW. The plasma density was raised steadily to the density limit by gas fuelling into the inner leg of the divertor at constant input power. Surprisingly, the onset of an X-point MARFE, which is precursor to the ultimate density limit [9], appears at about 15% lower density for the pulse with reversed field direction ($B\times\nabla B\uparrow$). The lower density limit in the $B\times\nabla B\uparrow$ case could be explained by the fact that the plasma is stable if at least one of the divertor legs is attached. For both field configurations, the inner leg detaches much earlier than the outer one and thus the outer divertor finally determines the density limit. The outer divertor in the reversed field discharge is colder than in forward field operation and correspondingly detaches earlier, what leads to lower density limit. Another possible explanation involves an increase of total radiation fraction (see Fig.3(d)) in the case with reversed field configuration. This effect of B_t-reversal on the density limit is consistent with earlier observations on ASDEX-Upgrade [10]. An increase of the density limit with input power was observed for both field directions.

The B_t direction has a substantial effect on the target density and temperature as well as on the detachment behaviour, as shown in Fig.1. The field reversal leads to an increase of the electron density at the outer strike point (OSP), and at the inner strike point (ISP) as well. Contrasting to the behaviour of the $B\times\nabla B\uparrow$ discharge, the I_s^{ISP} current to the inner divertor in forward field operation remains at a constant level to begin with, but falls strongly above $n_e \geq 2.5\times10^{19}\,m^{-3}$. This indicates that the inner divertor is partially detached from the start. At the same time the D_α emission in the inner divertor (see Fig.2) and neutral pressure in the divertor chamber (not shown) continues to increase, though, indicating plasma detachment [11]. In the $B\times\nabla B\uparrow$ case, the I_s^{ISP} current increases at first in the same way as I_s^{OSP} current and after about $n_e \geq 2.5\times10^{19}\,m^{-3}$ shows a continuously decreasing behaviour up to the discharge disruption. For high densities, $n_e \geq 2.7\times10^{19}\,m^{-3}$, in reversed configuration we observe nearly balanced electron temperatures and for $n_e \leq 2.7\times10^{19}\,m^{-3}$, the higher temperature side is inboard. Additionally, the degree of detachment (DoD) is included in this figure. The DoD is plotted for individual divertor Langmuir probes and is defined as $DoD = C\times\overline{n_n}^2 / I_s$ [11], where I_s is the ion saturation current of corresponding probe. The behaviour of the DoD at ISP for forward case confirmed the earlier statement about a detached inner leg from the beginning.

The inner qH divertor detachment for $B\times\nabla B\uparrow$ occurs later. Surprising is that, in contrast to the normal configuration ($B\times\nabla B\downarrow$), the outer scrape-off layer in reversed field operation detaches first and then follows the detachment at the separatrix (see Fig.1(g),(h)). The ion saturation current I_s^{OSP} to the outer divertor, measured by Langmuir probe at the strike point, initially increases for both field directions showing a factor of 2 larger values for pulse with ion ∇B drift direction away from the X-point. Shortly before the reversed field discharge disrupts, the I_s^{OSP} to the outer divertor drops dramatically: a MARFE forms, which leads to a 'density limit' disruption. In the forward field operation, the I_s^{OSP} current begins to decrease slowly at a density of $n_e = 3.3\times10^{19}m^{-3}$ which is much smaller than the density at onset of X-point MARFE ($n_e = 3.8\times10^{19}m^{-3}$).

Fig.2 shows the forward-reversed pairs of tomographic reconstruction of D_α- (top) and C III-emission (middle) as well the total radiation in the divertor region at two different electron densities: $n_e = 2.75\times10^{19}\,m^{-3}$ and $n_e = 3.3\times10^{19}\,m^{-3}$. In the early phase of both pulses, the maximum of the hydrogen radiation is located near the target plates at the position of the strike zone. In forward field discharge we expect significantly more radiation from the inner leg than from the outer. On the other hand, the reversed field configuration shows a more symmetrical D_α-emission distribution in the divertor region. This is due to an increase of the ion flux into the outer divertor with a simultaneous decrease of the electron temperature at target. With a reversal of the ion ∇B drift direction, the C III-emission in the outer leg decreases while increasing at the same time in the inner divertor. This is consistent with the behaviour of the T_e in the divertor: colder (warmer) outer (inner) leg leads to decrease (increase) of the physical sputtering of carbon. No significant changes are observed in the total radiation, between normal and reversed field direction plasmas. At $n_e = 3.3\times10^{19}m^{-3}$ D_α detaches from the inner divertor for the $B\times\nabla B\uparrow$ configuration, in the forward field pulse both legs are still attached. Also the CIII-emission in the $B\times\nabla B\downarrow$ case remains in attached condition at the OSP.

Comparison of experimental data relating to in-out divertor asymmetry is illustrated in Fig.3, which presents results of B_t-reversal on D_α-emission and CIII/D_α ratio as well as radiated power and power to the target. The left column of the figure presents the dependence of divertor asymmetry on density and the right column on the power entering to the SOL (P_{SOL}). In contrast to reversed field operation, in the discharges with the ion ∇B drift direction towards the X-point significantly higher asymmetries were observed. With B_t-reversal, the asymmetries in D_α and CIII emissions are substantially reduced from D_a^{in}/D_a^{out} =3.5 to $D_\alpha^{in}/D_\alpha^{out}$ =1.4 and from $(CIII/D_\alpha)^{in}/(CIII/D_\alpha)^{out}$=0.12 to $(CIII/D_\alpha)^{in}/(CIII/D_\alpha)^{out}$= 0.4 for n_e=2.7x10^{19}m^{-3}, and P_{NBI} = 1.8MW. The D_α-asymmetry in $B\times\nabla B\downarrow$ case is substantially suppressed at high densities and differs only slightly from the reversed field case. The CIII-asymmetry in reversed field discharge increases strongly with density and reaches the forward field value. In contrast to normal field operation, in reverse field regimes the asymmetries in D_α and CIII emissions do not depend significantly on the input power. Additionally, an increase of the radiation fraction is observed in the pulse with reversed

field (Fig.3(d)). The ratio of radiated power in the inner divertor to the power radiated in the outer divertor changes from 1.4 to 1.0 (more symmetrical in $B\times\nabla B\uparrow$ case) but at high densities no difference was observed. The right column of the Fig.3 summarises the result from experiments with normal and reversed pulses, in which the heating power was increased in steps. Fig.3(a) shows the ratio of the powers entering the outer and inner legs $P^{outer}_{div}/P^{inner}_{div}$, where P_{div} consists of the sum of power at the target (P_T) and the power radiated in a corresponding divertor leg ($P_{rad,div}^{in/out}$). At low power the $P^{outer}_{div}/P^{inner}_{div}$ ratio is less sensitive to the field reversal and varies between 1.5 and 2.0. However at high power the B_t-reversal effects strongly the $P^{outer}_{div}/P^{inner}_{div}$ ratio: the ratio increases for $B\times\nabla B\downarrow$ configuration up to value 2.3 while decreasing slightly to 1.25 with $B\times\nabla B\uparrow$. This behaviour contradicts the conclusion made in [12], where the out-in power asymmetry is explained by an asymmetry in divertor radiation. This statement may be relevant for operation with lower input power or in high density regime, where the $P_{rad,div}^{in/out}$ is comparable with power at the target. At higher input power though, divertor radiation cannot be significantly responsible for out-in power asymmetry. The target power asymmetries are probably a result of unequal power sharing between the targets, presumably due to classical drift effects [13]. The out-in power asymmetry (P_T^{out}/P_T^{in}) at target is very sensitive to the direction of the toroidal field, as shown in Fig.3(h). Its increases with P_{SOL} from 2.0 to 4.1 for $B\times\nabla B\downarrow$ while decreases slightly from 2.25 to 1.5 in reversed field configuration.

To understand the divertor asymmetry in forward and reversed field regimes, the EDGE2D/NIMBUS code [14], including all the classical particle drift terms was used. Poloidally and radially uniform transport coefficients were $D_\perp=0.5m^2/s$ and $\chi_\perp=1m^2/s$ for particle and energy respectively. Simulations with these coefficients produced good matches for both field directions with measured edge radial profile and temperature. Both physical [15] and chemical sputtering [16] control the intrinsic carbon content. As shown in Fig.3(h), calculated asymmetry increases with P_{SOL} in forward field case and decreases slightly in reversed field one, which matches well the experimental observation. The deviation between simulations and the experiment in the case of normal field operation could be explained by the fact that the code does not include heating of the divertor via radiation. Since the radiation, in first approximation, heats uniformly the inner and outer divertors, the P_T^{out}/P_T^{in} ratio becomes smaller. No significant differences are observed in $P_{rad}^{out}/P_{rad}^{in}$ ratio, between $B\times\nabla B\downarrow$ and $B\times\nabla B\uparrow$ causes, confirming that target asymmetry presumably due to drifts and not due to different radiation behaviour. Additionally, EDGE2D simulations successfully describe CIII-emission profiles, both for discharges with forward and reversed field directions. The D_α emission could be well predicted only for the attached divertor. On the other hand, EDGE2D cannot describe the detachment and, correspondingly, the D_α emission during detached divertor phase.

4. SUMMARY AND CONCLUSION

In JET, reversal effects of the toroidal field B_t on divertor plasma parameters were investigated in L-mode density limit discharges. The analysis of plasma parameters in the divertor for both forward

and reversed field discharges has led to the following conclusions:

- The density limit is approximately 15% lower in pulses with reversed B_t. An increase of the density limit with input power was observed for both field directions.
- Detachment behaviour in forward and reversed field pulses is very different. The inner divertor is detached from the start for normal field configuration. It detaches later in reversed field operations. In contrast to forward field operation, the outer SOL detaches first in discharges with ion ∇B direction away from the X-point, and the outer strike point detaches later.
- The radiation of D_α and CIII becomes more symmetrical with B_t–reversal and varies slightly with electron density.
- The total radiation in the divertor shows similar pattern structures for both field directions. There is a slight increase of radiation at X-point in the case of reversed field configuration. The out-in divertor asymmetry of total radiation cannot be fully responsible for out-in heat power asymmetry.
- EDGE2D calculations with drifts successfully describe CIII-emission profiles as well as out-in target heat power asymmetry, both for discharges with forward and reversed field directions.

REFERENCES

[1]. F. Wagner, M. Keilhacker and the ASDEX and NI Teams, J. Nucl. Mater. 121 (1984) 103.

[2]. D. N. Hill.et al., J. Nucl. Mater. 176-177 (1990) 158.

[3]. K. Itami, M. Shimada and N. Hosogane, J. Nucl. Mater. 196-198 (1992) 755.

[4]. N. Asakura et al., J. Nucl. Mater. 220-222 (1995) 395.

[5]. I. H. Hutchinson et al, Plasma Phys. Control. Fusion 38 (1996), A301.

[6]. R. Reichle et al., Proc. 18th Europ. Conf. On Controlled Fusion and Plasma Physics, vol. III (EPS,Berlin, 1991) 105.

[7]. A.V. Chankin et al., Plasma Phys. Control. Fusion 38 (1996), 1579.

[8]. A. Huber et al., J. Nucl. Mater. 313-316 (2003) 925.

[9]. H.Y. Guo et al., Nucl. Fusion 40 (2000), 379.

[10]. V. Mertens et al., Plasma Phys. Control. Fusion 36 (1994), 1307.

[11]. A. Loarte et al., Nucl. Fusion 38 (1998), 331.

[12]. C.S. Pitcher and P. C. Stangeby, Plasma Phys. Control. Fusion 39 (1997), 779.

[13]. W. Fundamenski et. al., this conference.

[14]. R. Simonini et al., Contrib. Plasma Phys. 34 (1994) 368.

[15]. W. Eckstein et al., Report IPP9/82, Max-Planck-Institut für Plasmaphysik, Garching (1993)

[16]. A.A. Haasz et al., J. Nucl. Mat. 248 (1997), 19

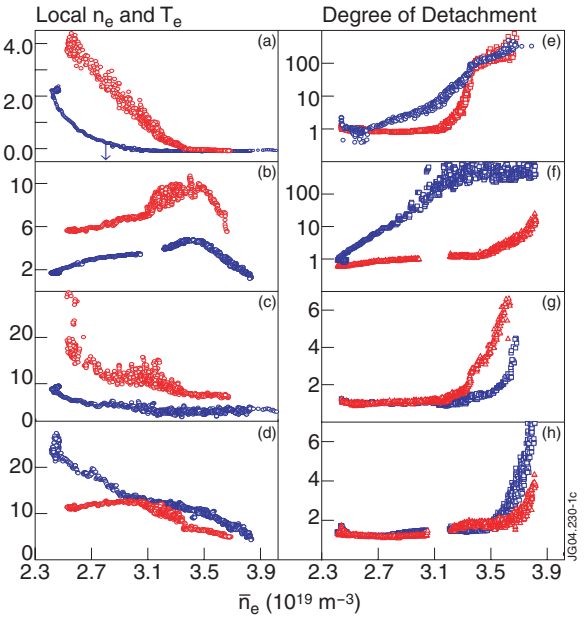

Figure 1: Characteristics of the MkIIGB-SRP divertor plasma for both field directions as function of $\bar{n}_e$: (left column) electron density and temperature at Inner (ISP) and Outer (OSP) Strike Points; (right column) the degree of detachment (DoD) of individual probes for both divertor legs.

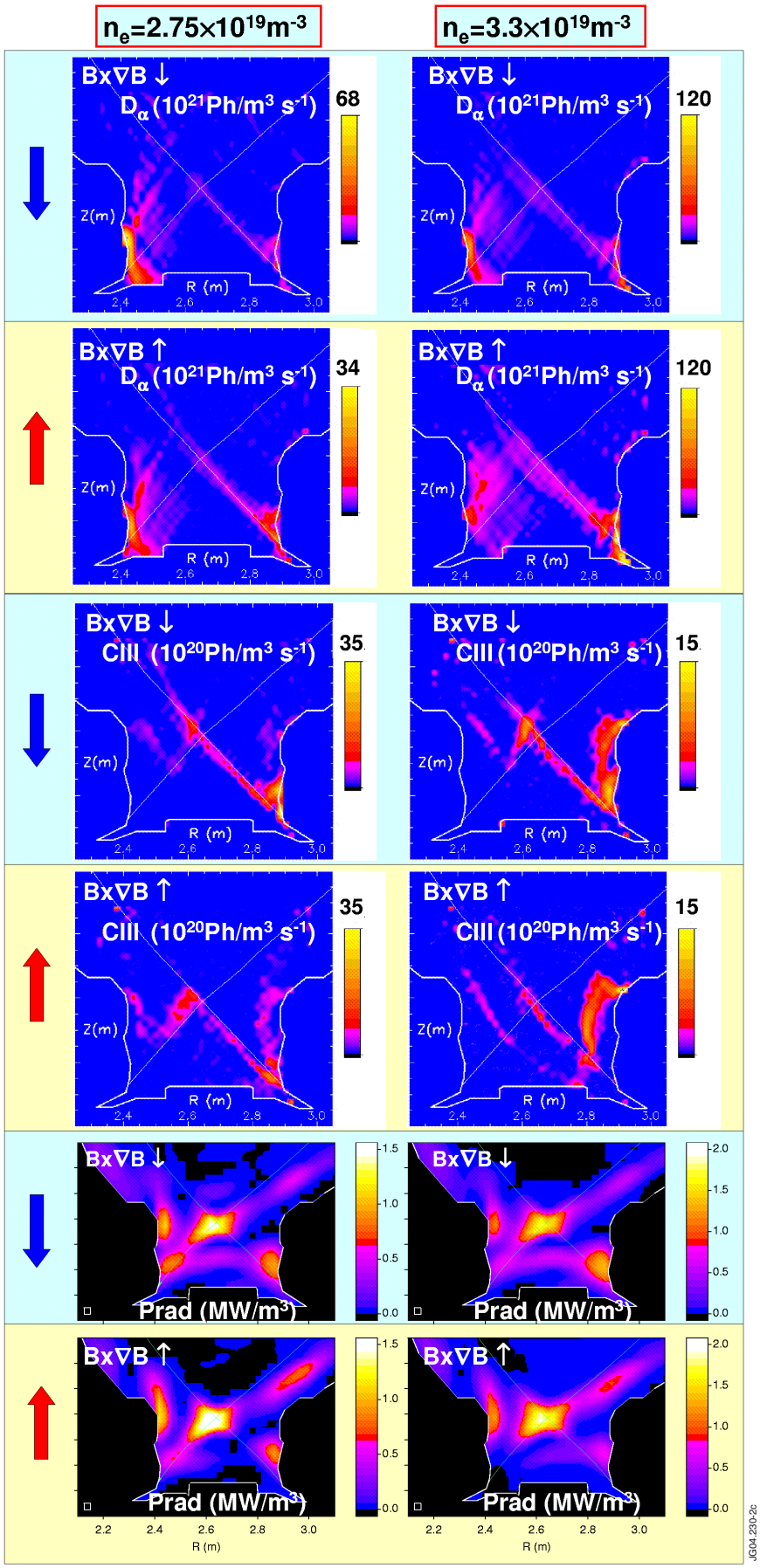

Figure 2: Tomographic reconstruction of D_α- (upper rows) and C°III-emission (middle rows) as well the reconstruction of total radiated power (lower rows) in the divertor region at two central averaged densities for both field directions.

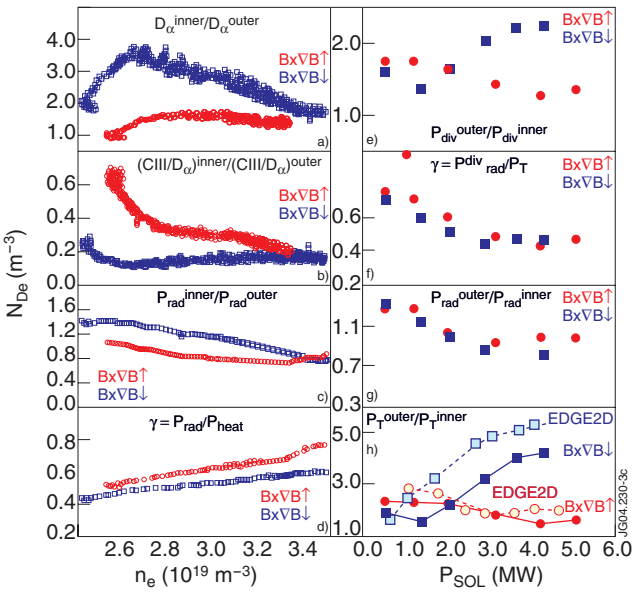

Figure 3: Characteristics of divertor asymmetry versus $\bar{n}_e$ (left column) and power entering the SOL (right column) for forward and reversed field directions.